Broadband and Precise Microwave Time Reversal Using a Single Linearly Chirped Fiber Bragg Grating

Jiejun Zhang, *Student Member, IEEE*, and Jianping Yao, *Fellow, IEEE*

***Abstract*—We propose and experimentally demonstrate a novel technique to achieve broadband and precise microwave time reversal using a single linearly chirped fiber Bragg grating (LCFBG). In the proposed approach, the time reversal is realized by the LCFBG that is operating in conjunction with a polarization beam splitter (PBS) to enable a triple use of the LCFBG with the microwave waveform entering the LCFBG from either the long or the short wavelength end. Since the LCFBG has a wide bandwidth and is used three times with exactly complementary and identical dispersion, broadband and precise microwave time reversal is ensured. A theoretical analysis is performed which is validated by simulations and an experiment. The time reversal of three different microwave waveforms with a bandwidth over 4 GHz and a time duration of approximately 10 ns is demonstrated.**

***Index Terms*—Microwave conjugator, microwave photonics, photonic microwave signal processing, temporal pulse shaping, time reversal.**

I. Introduction

TIME reversal, also known as phase conjugation in optics, is a technique widely used to increase the resolution of a detection system. Using time reversal, the energy of a signal can be focused in a detection system with a resolution that is much higher than the value of the signal wavelength [1]–[3]. In an acoustic time reversal system [4], for example, a short acoustic pulse is sent from a source that propagates through a complex medium and is captured by a transducer array. The recorded signal is digitized, time reversed digitally, and then transmitted. Recently, an optical time reversal system was implemented to focus a lightwave signal through a scattering medium [5]. In 2004, time reversal of an microwave signal was proposed to overcome the multipath problem for microwave communications [6]. It is shown that time reversal is not only capable of solving the multipath problem, but it can also control the microwave power distribution by focusing more power to the detector, which has been theoretically and experimentally verified in [7] and [8]. Since then, microwave time reversal has attracted significant research interests due to its promising applications in microwave imaging and microwave communication. A microwave imaging system with a significantly improved resolution by time reversal was proposed for breast cancer detection [9], [10]. In [11]–[13], microwave time reversal was used for hyperthermia treatment of cancer thanks to its capability to focus electromagnetic power. A microwave super-resolution system was demonstrated in [14], in which time reversal was used to focus a microwave signal with a resolution of one thirtieth of the microwave wavelength, a value that is beyond the diffraction limit. In [15], it was demonstrated that, using time reversal, the phase distortion of a UWB signal in a communications system can be effectively compensated.

It is similar to acoustic time reversal, to implement microwave time reversal, digital solutions are usually employed, which involve analog-to-digital conversion (ADC), digital signal processing (DSP), and digital-to-analog conversion (DAC). In a laboratory environment, these functions were implemented using a real-time oscilloscope to perform sampling, a computer to perform DSP, and an arbitrary waveform generator to perform DAC [15]. The key limitations of a digital microwave time reversal system are the relatively slow speed and small bandwidth and are only suitable for signal processing with a frequency and bandwidth of a few gigahertz. For example, the bandwidths of the digital microwave time-reversal systems are only 2 MHz [6], 20 MHz [10], and 150 MHz [7]. In [15], a pulse with an effective bandwidth of 9.6 GHz was generated, but at the cost of a very expensive electronic arbitrary waveform generator (AWG). For many applications such as radar and high-speed communications, however, time reversal of a high-frequency and wideband microwave signal is highly demanded. It has been theoretically proved that time reversal of a microwave signal with a wider bandwidth can significantly improve the focusing efficiency of a microwave imaging system [16]. Photonic solutions have been proposed to implement high-frequency and wideband microwave time reversal. In [17], microwave time reversal was optically realized by using the three photon echo effect in an erbium-doped YSO crystal. An unprecedented time duration of 6 μs was demonstrated. The application of the time reversal in a temporal imaging system was discussed in [18]. Despite the extremely long time duration, the bandwidth of the time reversal was limited only to 10 MHz, which is small and could be easily achieved by a digital time-reversal system. In [19], a microwave photonic system to achieve broadband microwave time reversal using a temporal pulse shaping system was proposed. Theoretically, the bandwidth can be as large as 18 GHz. However, since two independent dispersive elements were used in the system, a relatively large dispersion mismatch between the two dispersive

Manuscript received November 16, 2014; revised March 05, 2015 and May 04, 2015; accepted May 07, 2015. Date of publication June 01, 2015; date of current version July 01, 2015. This work was supported by the Natural Science and Engineering Research Council (NSERC) of Canada. The work of J. Zhang was supported in part by the China Scholarship Council (CSC).

The authors are with the Microwave Photonics Research Laboratory, School of Electrical Engineering and Computer Science, University of Ottawa, Ottawa, ON K1N 6N5, Canada (e-mail: jpyao@eecs.uottawa.ca).

Color versions of one or more of the figures in this paper are available online at http://ieeexplore.ieee.org.

Digital Object Identifier 10.1109/TMTT.2015.2432016

elements resulted, which led to large waveform distortions with a reduced system performance (defocusing).

In this paper, we propose and experimentally demonstrate a microwave photonic system to realize time reversal of a microwave waveform with a high operation frequency and a large bandwidth by using a single LCFBG. This is a continuation of our recent work reported in [20] where the temporal duration of the time-reversed waveform was small. The time reversal reported in this paper is realized by using a long and wideband LCFBG that is operating in conjunction with a polarization beam splitter (PBS) to enable a triple use of the LCFBG with the optical waveform entering from either the long or the short wavelength end. Since the LCFBG is used three times with exactly complementary (the first two times) and identical (the last two times) dispersion, a precise microwave time reversal is ensured. In addition, the LCFBG has a large bandwidth, thus high frequency and broadband microwave operation is also ensured.

The proposed technique is analyzed theoretically and verified by simulations in Section II. A proof-of-concept experiment by using three different microwave waveforms with a bandwidth up to 4 GHz and a time duration of approximately 10 ns is presented in Section III. A conclusion is drawn in Section IV.

II. Principle

A. System Configuration

Fig. 1 shows the proposed microwave photonic system for broadband and precise microwave time reversal. A transform-limited optical pulse generated by a mode-locked laser (MLL) is filtered by a bandpass optical filter (OF) with a bandwidth of 4 nm and sent to the LCFBG from its long wavelength end via a three-port optical circulator (OC1). The optical pulse is then temporally stretched by the LCFBG. The LCFBG has a reflectivity of over 95% and a bandwidth of 4 nm, which is equal to the spectral width of the optical pulse from the OF. Hence, the optical pulse from the OF is almost completely reflected by the LCFBG and the transmission is small and negligible. At the third port of OC1, a Mach–Zehnder modulator (MZM) is connected, to which a microwave waveform to be temporally reversed is applied. A polarization controller (PC1) is incorporated between OC1 and the MZM to align the polarization state of the optical pulse to the principal axis of the MZM to minimize the polarization-dependent loss. At the output of the MZM, the optical pulse is directed into a four-port optical circulator (OC2). A PBS is used to connect the short wavelength end of the LCFBG to the second and third ports of OC2. Two other PCs (PC2 and PC3) are employed between the PBS and OC2 to control the polarization directions of the light waves to the PBS, so that the light waves can be efficiently coupled to the LCFBG by the PBS. The optical pulse injected to the first port of OC2 is directed to the second port and then sent to the short wavelength end of the LCFBG through the PBS. The optical pulse is then dispersed by the LCFBG and returned to the PBS. Since there is no Faraday Effect involved in this process, the return light should have the polarization that perfectly matches the polarization of the lower arm of the PBS. Hence, the pulse is completely reflected to the second port of OC2. At the third port of OC2, an identical process occurs and the pulse is dispersed again at the short wavelength end of the LCFBG. The joint operation of OC2 and the PBS allows the optical pulse from the MZM to be independently and temporally dispersed by the LCFBG twice. The optical pulse is finally detected by a photodetector (PD) connected to the fourth port of OC2 and a time-reversed microwave waveform is obtained at the output of the PD, which is monitored by a real-time oscilloscope.

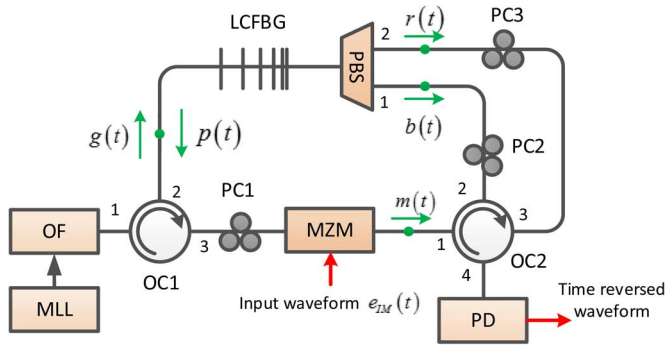

Fig. 1. Schematic of the proposed microwave time-reversal system. MLL: mode-locked laser; OF: optical filter; LCFBG: linearly chirped fiber Bragg grating; PC: polarization controller; MZM: Mach–Zehnder modulator; PBS: polarization beam splitter; PD: photodetector; OC: optical circulator.

B. Time-Reversal Modeling

Mathematically, the LCFBG can be modeled as a linear and time-invariant (LTI) system with a quadratic phase response and unity amplitude response. Assuming that the electrical field of the optical pulse from the OF is $g(t)$, after being dispersed by the LCFBG (entering from the long wavelength end), the electrical field of the optical pulse at the third port of OC1 is given by [21]

$$p(t) = g(t) * \exp\left(j\frac{t^2}{2\ddot{\Phi}}\right) \tag{1}$$

where $\ddot{\Phi}$ is the dispersion coefficient of the LCFBG looking into it from the long wavelength end, and $*$ denotes the convolution operation.

Note that the dispersion coefficient looking into the LCFBG from the short wavelength end is $-\ddot{\Phi}$. Fig. 2 shows the reflection spectrum of an LCFBG fabricated based on the holographic method in a single-mode fiber with a length of 1 m. The spectrum is measured by an optical vector analyzer (OVA, Luna Technologies). As can be seen, the LCFBG has a bandwidth of 4 nm and a central wavelength of 1551.4 nm, which is approximately equal to the central wavelength of the pulse spectrum from the OF. The group delay responses of the LCFBG measured from its short and long wavelength ends are also shown in Fig. 2. As can be seen that the group delay responses are complementary and the dispersion coefficients are $+2500$ ps/nm and -2500 ps/nm, corresponding to the green and red lines, respectively. Since the LCFBG has a long length, which is more than the measurable length of the OVA, in the measurement the LCFBG is considered as four cascaded subsections, and each subsection is measure independent. The spectrum of the entire

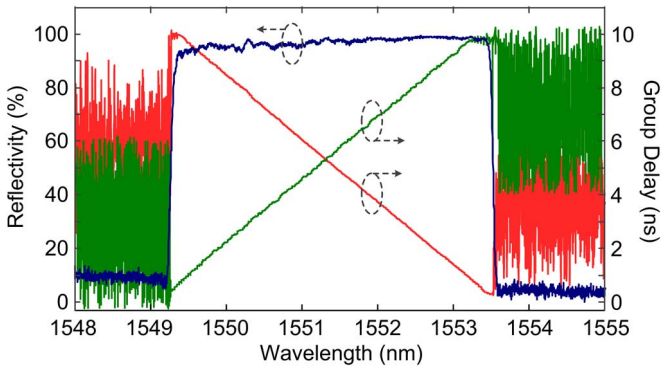

Fig. 2. Reflection spectrum and group delay responses of the LCFBG.

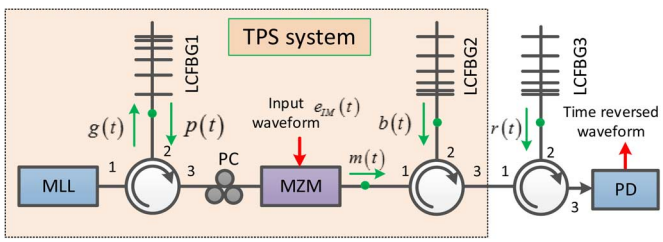

Fig. 3. Implementation of the proposed microwave time-reversal system using three LCFBGs.

LCFBG is then achieved by synthesizing the four measurements corresponding to the spectra of the four subsections.

The microwave time-reversal system can be modeled as a temporal pulse shaping (TPS) system [17] with a pair of complementary dispersive elements of $\ddot{\Phi}$ and $-\ddot{\Phi}$, followed by a residual dispersion of $-\ddot{\Phi}$, as shown in Fig. 3. As can be seen, the implementation of the system based on our proposed configuration in Fig. 1 to use only a single LCFBG will significantly reduce the complexity and improve the performance (with no dispersion mismatch).

The electrical field at the output of the MZM is given by

$$m(t) = p(t) \times e_{IM}(t) \tag{2}$$

where $e_{IM}(t)$ is the microwave signal applied to the MZM.

After being dispersed by the LCFBG entering from the short wavelength end of the LCFBG for the first time, the electrical field becomes

$$b(t) = m(t) * \exp\left(j\frac{t^2}{-2\ddot{\Phi}}\right). \tag{3}$$

If the duration of the MLL pulse τ_0 and the dispersion of LCFBG satisfy the far field condition $|\tau_0^2/\ddot{\Phi}| \ll 1$, the Fraunhofer approximation can be adopted. Substituting (1) and (2) into (3), we have [22], [23]

$$b(t) \propto g(t) * E_{IM}(\omega)|_{\omega=\frac{t}{\ddot{\Phi}}} \tag{4}$$

where $E_{IM}(\omega)$ is the Fourier transform of $e_{IM}(t)$.

The electrical field at the output of the entire time-reversal system $r(t)$ is obtained by propagating the optical signal $b(t)$ from the temporal pulse shaping system through a third dispersive element with a value of residual dispersion of $-\ddot{\Phi}$ via the fourth port of OC2 [21]

$$r(t) = \exp\left(\frac{jt^2}{-2\ddot{\Phi}}\right) B(\omega)|_{\omega=\frac{t}{-\ddot{\Phi}}} \tag{5}$$

where $B(\omega)$ is the Fourier transform of $b(t)$.

Substitute (4) into (5), we have

$$\begin{aligned} r(t) &= \exp\left(\frac{jt^2}{-2\ddot{\Phi}}\right) F\left[g(t) * E_{IM}\left(\frac{t}{\ddot{\Phi}}\right)\right]\Big|_{\omega=\frac{t}{-\ddot{\Phi}}} \\ &= \exp\left(-\frac{jt^2}{2\ddot{\Phi}}\right) G(\omega)\frac{|\ddot{\Phi}|}{2\pi} e_{IM}(\ddot{\Phi}\omega)\Big|_{\omega=\frac{t}{-\ddot{\Phi}}} \\ &= \frac{|\ddot{\Phi}|}{2\pi}\exp\left(-\frac{jt^2}{2\ddot{\Phi}}\right) G\left(-\frac{t}{\ddot{\Phi}}\right) e_{IM}(-t) \end{aligned} \tag{6}$$

where $G(\omega)$ is the Fourier transform of $g(t)$.

The optical pulse at the fourth port of OC2 is detected by the PD. The generated photocurrent is given by

$$I(t) = \Re\,|r(-t)|^2 \propto G^2\left(-\frac{t}{\ddot{\Phi}}\right) e_{IM}^2(-t) \tag{7}$$

where $\Re$ is the responsivity of the PD.

C. Waveform Distortion

As can be seen from (7), the microwave waveform at the output of the system is a time-reversed version of the input signal except for a multiplying term $G_2(-t/\ddot{\Phi})$. Ideally, the optical pulse from the MLL is ultrashort, and its temporally dispersed version is ultrawide and flat, which will have small impact on the generated waveform. To study the impact of $G_2(-t/\ddot{\Phi})$ on the generated time-reversed waveform, a simulation is performed in which the dispersive element is a real LCFBG which has a spectral response given in Fig. 2. An up-chirped microwave waveform shown in Fig. 4 (solid line) is used as the input signal $e_{IM}(t)$. The microwave waveform at the output of the PD is frequency down-chirped, which is a time-reversed version of the input waveform, except for a slowly varying envelope due to $G(-t/\ddot{\Phi})$. In the simulation, $G(-t/\ddot{\Phi})$ is the optical spectrum of an optical pulse from the MLL after being filtered by the bandpass OF and reflected three times by the LCFBG. From Fig. 4, it can be seen that the output waveform has exactly the same temporal duration and shape as compared with the input microwave waveform. Note that, to ease the comparison, the generated time-reversed waveform is flipped horizontally and shown in the same figure. A correlation coefficient [24] of 0.998 is achieved between the original and time-reversed signals. The very small envelope distortion is induced by $G_2(-t/\ddot{\Phi})$, which can be further suppressed by using an MLL with a flatter optical spectrum and an LCFBG with more uniform reflectivity.

D. Electrical Bandwidth Limit

The limited bandwidth is another factor that may influence the performance of the time-reversal operation. In the proposed system, the bandwidth of the LCFBG is very wide, and the

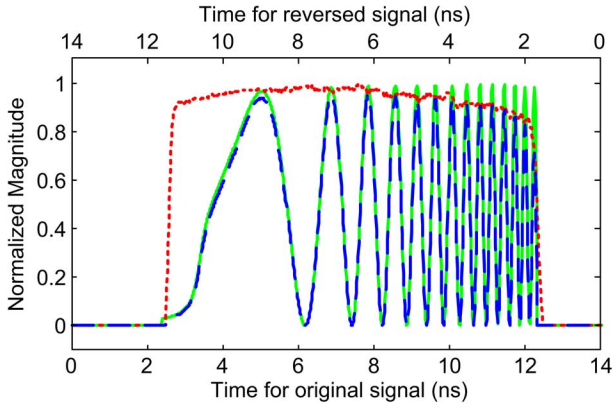

Fig. 4. Simulated time-reversed waveform considering the impact from $G_2(-t/\ddot{\Phi})$. Dotted line: input up-chirped waveform; dashed line: time-reversed output waveform with a frequency down-chip; solid: the profile of $G_2(-t/\ddot{\Phi})$, determined by the spectrum of the optical pulse from the MLL and the dispersion of the LCFBG.

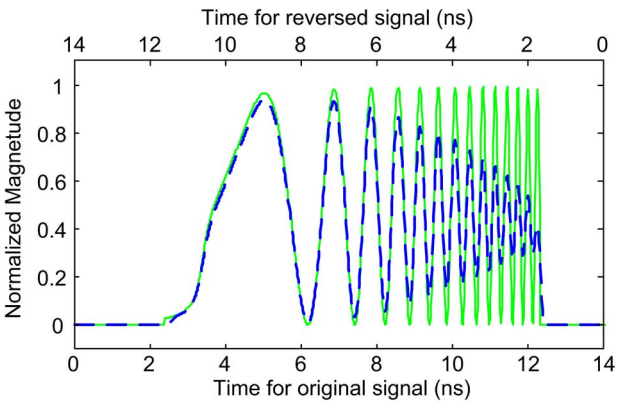

Fig. 5. Simulated time-reversed waveform when the limited bandwidth of the electronic components is considered. Solid line: input chirped signal; dashed line: output time-reversed signal for a limited electronic bandwidth of 4 GHz.

system bandwidth is mainly limited by the electronic components used, including the electronic amplifiers, MZM, and the PD. Fig. 5 shows the distortion caused by the limited electronic bandwidth. Similar to Fig. 4, a frequency up-chirped waveform is used as the input waveform. At the output, a time-reversed waveform with a reduced amplitude is observed, especially for high-frequency components, when a low-pass filter (3-dB cutoff frequency at 4 GHz) is employed to emulate the bandwidth limitation of the electronic components. The correlation coefficient between the original and the time-reversed waveforms is 0.981. As the central frequency of the input signal increases, the correlation coefficient drops drastically, indicating a largely degraded performance of the system. Again, to ease the comparison, the generated time-reversed waveform is flipped horizontally and also shown in Fig. 5. Since high-speed MZMs and PDs with a bandwidth up to 100 GHz or higher are now commercially available, the electronic bandwidth of the time-reversal system may not be limited by the electronic components. Then, the bandwidth of the time-reversal system will be determined by the optical components. Theoretically, the LCFBG is the only optical component with a finite bandwidth. Its bandwidth may limit the bandwidth of the time-reversal system.

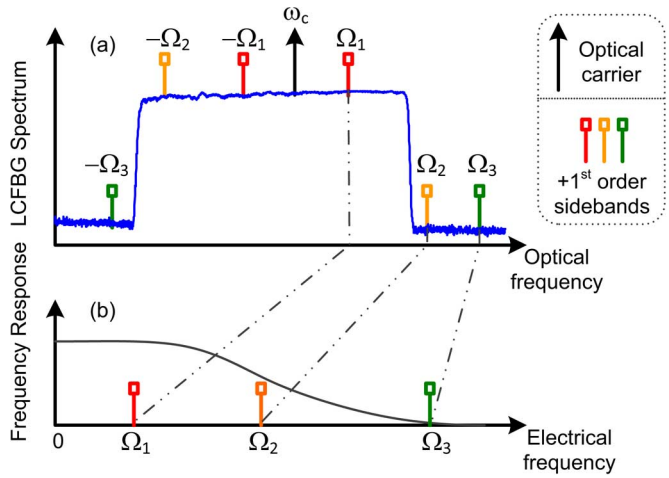

Fig. 6. Mechanism for the bandwidth limit of the optical part. (a) Optical carrier ω_c and sidebands reflected by the LCFBG. As modulation frequency increases from ω_1 to ω_3, the sidebands may locate outside the reflection band of LCFBG. (b) Corresponding frequency response of the LCFBG.

E. Photonic Bandwidth Limit

For an intensity-modulation and direct-detection (IM/DD) system, when a microwave signal is modulated on an optical carrier, first-order optical sidebands will be generated. The beating between the optical carrier and the sidebands at a PD will recover the modulation microwave waveform. When a temporally stretched MLL pulse is used as an optical carrier, however, the modulation process will broaden the optical spectrum. When the broadened spectrum exceeds the bandwidth of the LCFBG, the microwave power detected at the PD will decrease since some of the spectral components will not be reflected, resulting in a limited bandwidth of the time reversal system.

Fig. 6 illustrates the impact of the limited bandwidth of the LCFBG on the microwave detection. First, we assume a single-frequency optical carrier at ω_c that is modulated by a microwave signal at a relatively low frequency Ω_1. Due to the low microwave frequency, the two sidebands are within the reflection band of the LCFBG, as shown in Fig. 6(a). Both of them will be reflected and beat with the optical carrier at the PD, thus a maximum microwave power is achieved. When the microwave signal is increased to a higher frequency ω_2, only one sideband is within the LCFBG reflection band, and the power of the microwave beat signal at the PD will be reduced by half. Finally, as the modulation frequency is increased to Ω_3, no sidebands fall within the LCFBG reflection band, and thus no microwave signal will be detected. Therefore, the frequency response of the system corresponds to a low-pass filter with its frequency response shown in Fig. 6(b).

We then quantitatively calculate the bandwidth of the system due to the finite the bandwidth of the LCFBG. Since intensity modulation is used, the detected microwave power should be the summation of the powers of the beat signals between the optical carrier and its two first-order sidebands as follows:

$$P(\omega_c, \Omega) \propto R(\omega_c) \cdot R(\omega_c + \Omega) + R(\omega_c) \cdot R(\omega_c - \Omega) \quad (8)$$

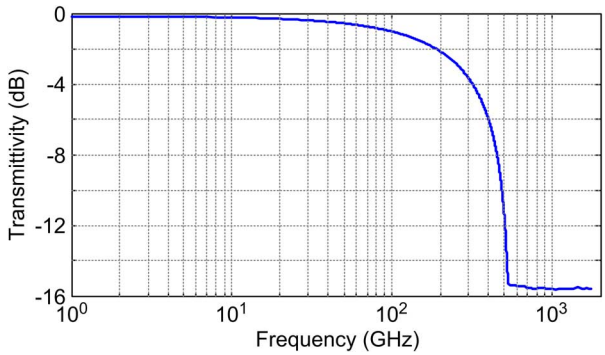

Fig. 7. Microwave spectral response of the time-reversal system due to the finite bandwidth of the LCFBG.

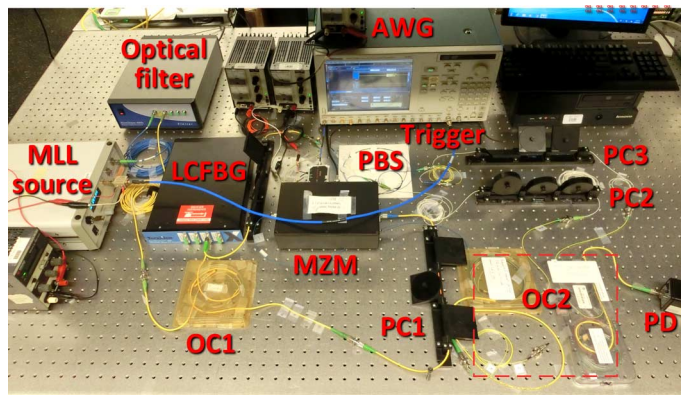

Fig. 8. Photograph of the experiment setup. Two three-port circulators are cascaded to function as a four-port circulator OC2.

where $R(\omega)$ is the reflectivity of the LCFBG. Since all of the spectral components of the optical pulse from the MLL over a frequency range of $\delta\omega$ contribute to the optical carrier, the total microwave power detected at the PD is

$$P(\Omega) = \int_{\delta\omega} P(\omega_c, \Omega) d\omega_c. \tag{9}$$

Based on (9) and using the measured LCFBG reflection spectrum shown in Fig. 2, the microwave spectral response of the time-reversal system is calculated. As shown in Fig. 7, the system is a low-pass filter with the 3-dB cutoff frequency at 273 GHz, which is approximately equal to half of the optical bandwidth of the LCFBG.

III. Experiment

An experiment based on the setup shown in Fig. 1 is performed. An optical pulse from the wavelength tunable MLL (PriTel FFL-1550-20) with a 3-dB bandwidth of 8 nm and a pulse width less than 600 fs is used as the light source. The repetition rate of the pulse train from the MLL is 20 MHz. An OF with a bandwidth of 4 nm centered at the spectrum of the MLL is employed to achieve a flat spectrum and, at the same time, to ensure that the pulse can be completely reflected by the LCFBG. The LCFBG was fabricated using the holographic method. A microwave arbitrary waveform generator (Tektronix AWG7102) with a sampling rate of 10 Gb/s is used to generate a microwave waveform that is applied to the MZM (JDSU OC-192, bandwidth of 10 GHz) after amplified by an electrical amplifier (MTC5515, bandwidth of 10 GHz). The microwave waveform and the optical pulse from the MLL are synchronized by applying a trigger signal from the MLL to the arbitrary waveform generator. The optical pulse at the fourth port of OC2 is a time-reversed optical waveform as compared with the optical waveform at the output of the MZM. The time-reversed optical waveform is applied to the PD (New Focus 1414, 25 GHz). The detected waveform is monitored by a 32-GHz real-time oscilloscope (Agilent 93204A). A photograph of the experimental setup is shown in Fig. 8.

The key device to achieve the time reversal is the LCFBG, which is fabricated in a single-mode fiber with a length of 1 m. The reflection spectrum and the group delay responses are shown in Fig. 2.

It can be calculated that the optical pulse from the OF is stretched to have a time duration of $\tau = \ddot{\Phi} \times \Delta\lambda = 10$ ns at the input of the MZM. Hence, the time duration of the input microwave signal should be limited to 10 ns in order to be carried by the temporally dispersed optical pulse. The time duration of the pulse at the output of the OF is estimated to be 0.88 ps, which satisfies the far-field condition for a TPS system [21]. Note that the far-field condition does not need to be considered when the pulse passing through the LCFBG for the second and third times [25].

Three different waveforms are generated by the arbitrary waveform generator to test the operation of the proposed microwave time-reversal system. The three waveforms are a sawtooth wave, a chirped wave, and an arbitrary waveform. To compare an original waveform and a time-reversed waveform simultaneously, a 3-dB coupler was used after the MZM to direct part of the modulated optical pulse to a PD and sampled by another channel of the real-time oscilloscope.

Fig. 9 shows the microwave waveforms from the two separate channels of the real-time oscilloscope, which correspond to the waveforms before and after the time reversal. Specifically, in Fig. 9(a), a three-cycle up-ramp sawtooth is time reversed to become a down-ramp sawtooth. A small amplitude change in the three cycles can be observed, which is caused by the nonideally flat spectrum shape of the MLL pulse, as confirmed by the simulation. The amplitude change can be reduced by improving the flatness of the optical pulse. In Fig. 9(b), a frequency up-chirped microwave waveform with a time duration of 10 ns and a frequency range from dc to 4 GHz is time reversed to become a frequency down-chirped waveform. Note that the input microwave waveform is not an ideal frequency-chirped pulse due to the limited sampling rate (10 Gb/s) of the arbitrary waveform generator, and the limited bandwidth of the EA and the MZM. In Fig. 9(c), an arbitrary waveform is generated by the arbitrary waveform generator which is also time reversed. It can be seen from Fig. 9(a)–(c) that the time-reversed waveforms have exactly the same time duration and the same shape with the original waveforms, except for very small amplitude distortions caused by the limited bandwidth of the electronic components and the non-flat spectral shape of the optical pulse. By correlating the original waveforms with a flipped version of

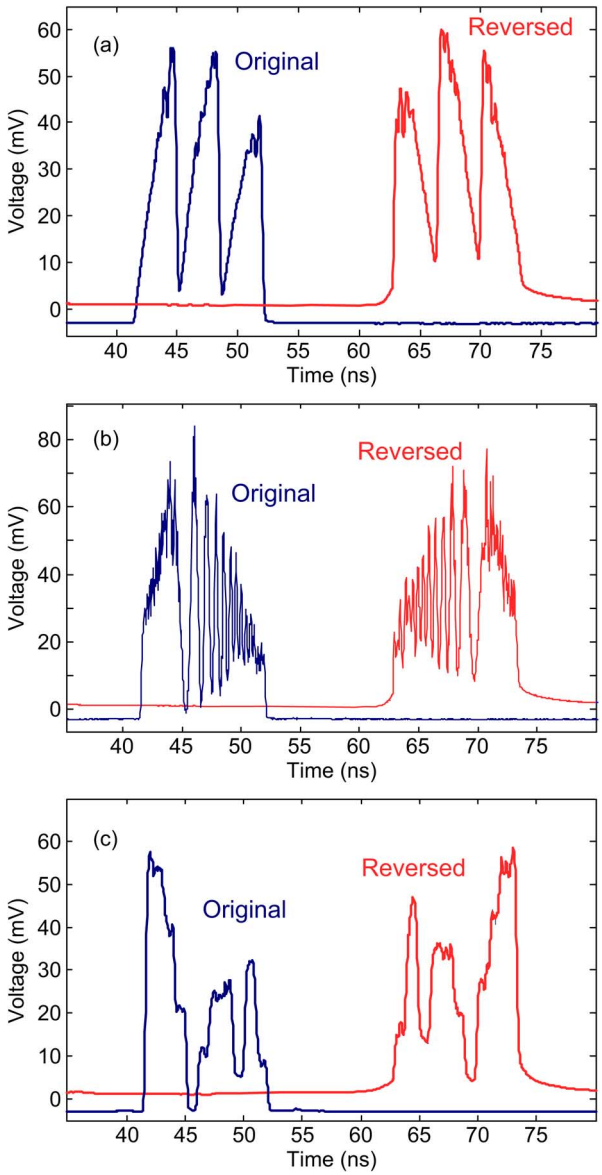

Fig. 9. Comparison between the original and the time-reversed waveforms. (a) Sawtooth wave. (b) Chirped wave. (c) Arbitrary waveform. The corresponding correlation coefficients are calculated to be 0.930, 0.939, and 0.951.

the time-reversed waveforms, we have three correlation coefficients of 0.930, 0.939, and 0.951, which are slightly smaller than the theoretical values of 1 due to the existence of system noise. Nevertheless, precise and single-shot time reversal of a microwave waveform with a bandwidth up to 4 GHz and a time duration of 10 ns has been achieved.

IV. Conclusion

We have proposed and experimentally demonstrated a novel technique to achieve broadband and precise real-time microwave time reversal using a single LCFBG. The key advantage of the proposed technique was the use of only a single LCFBG, which was used three times, and thus the system was greatly simplified. More importantly, the triple use of the LCFBG enabled the complete elimination of the dispersion mismatch existing in a time-reversal system using three independent dispersive elements. The proposed technique was studied theoretically and validated by an experiment. The time reversal of three different microwave waveforms with a bandwidth of 4 GHz and a time duration of about 10 ns was demonstrated. To further increase the time duration, a dispersive element with a greater time delay is needed, for example, a longer LCFBG, or a dispersive filter near atomic resonance in rare-earth ion-doped crystals.

Acknowledgment

The authors would like to thank TeraXion for providing the linearly chirped fiber Bragg grating used in the experiment.

References

[1] J. M. Moura and Y. Jin, "Detection by time reversal: Single antenna," *IEEE Trans. Signal Process.*, vol. 55, no. 1, pp. 187–201, Jan. 2007.
[2] G. Borzdov, "Localized electromagnetic and weak gravitational fields in the source-free space," *Phys. Rev. E*, vol. 63, Feb. 2001, Art. ID 036606.
[3] D. H. Chambers and J. G. Berryman, "Time-reversal analysis for scatterer characterization," *Phys. Rev. Lett.*, vol. 92, no. 2, Jan. 2004, Art. ID 023902.
[4] W. Kuperman, W. S. Hodgkiss, H. C. Song, T. Akal, C. Ferla, and D. R. Jackson, "Phase conjugation in the ocean: Experimental demonstration of an acoustic time-reversal mirror," *J. Acoust. Soc. Amer.*, vol. 103, no. 1, pp. 25–40, Jan. 1998.
[5] E. H. Zhou, H. Ruan, C. Yang, and B. Judkewitz, "Focusing on moving targets through scattering samples," *Optica*, vol. 1, no. 4, pp. 227–232, Oct. 2014.
[6] G. Lerosey, J. De Rosny, A. Tourin, A. Derode, G. Montaldo, and M. Fink, "Time reversal of electromagnetic waves," *Phys. Rev. Lett.*, vol. 92, no. 19, May 2004, Art. ID 193904.
[7] G. Lerosey, J. De Rosny, A. Tourin, A. Derode, and M. Fink, "Time reversal of wideband microwaves," *Appl. Phys. Lett.*, vol. 88, no. 15, Apr. 2006, Art. ID 154101.
[8] J. de Rosny, G. Lerosey, and M. Fink, "Theory of electromagnetic time-reversal mirrors," *IEEE Trans. Antennas Propag.*, vol. 58, no. 10, pp. 3139–3149, Oct. 2010.
[9] P. Kosmas and C. M. Rappaport, "Time reversal with the FDTD method for microwave breast cancer detection," *IEEE Trans. Microw. Theory Techn.*, vol. 53, no. 7, pp. 2317–2323, Jul. 2005.
[10] P. Kosmas and C. M. Rappaport, "FDTD-based time reversal for microwave breast cancer detection-localization in three dimensions," *IEEE Trans. Microw. Theory Techn.*, vol. 54, no. 4, pp. 1921–1927, Apr. 2006.
[11] B. Guo, L. Xu, and J. Li, "Time reversal based microwave hyperthermia treatment of breast cancer," in *Proc. IEEE 39th Asilomar Conf. Signals, Syst. Comput.*, Oct. 2005, pp. 290–293.
[12] H. D. Trefná, J. Vrba, and M. Persson, "Time-reversal focusing in microwave hyperthermia for deep-seated tumors," *Phys. Med. Biol.*, vol. 55, no. 8, pp. 2167–2185, Mar. 2010.
[13] P. Kosmas, E. Zastrow, S. C. Hagness, and B. D. Van Veen, "A computational study of time reversal techniques for ultra-wideband microwave hyperthermia treatment of breast cancer," in *Proc. IEEE/SP 14th Workshop on Statistical Signal Process.*, , Aug. 2007, pp. 312–316.
[14] G. Lerosey, J. De Rosny, A. Tourin, and M. Fink, "Focusing beyond the diffraction limit with far-field time reversal," *Science*, vol. 315, no. 5815, pp. 1120–1122, Feb. 2007.
[15] A. Dezfooliyan and A. M. Weiner, "Experimental investigation of UWB impulse response and time reversal technique up to 12 GHz: Omnidirectional and directional antennas," *IEEE Trans. Antennas Propag.*, vol. 60, no. 7, pp. 3407–3415, Jul. 2012.
[16] A. Derode, A. Tourin, and M. Fink, "Random multiple scattering of ultrasound. II. Is time reversal a self-averaging process?," *Phys. Rev. E*, vol. 64, Aug. 2001, Art. ID 036606.
[17] H. Linget, L. Morvan, J.-L. Le Gouët, and A. Louchet-Chauvet, "Time reversal of optically carried radiofrequency signals in the microsecond range," *Opt. Lett.*, vol. 38, no. 5, pp. 643–645, Mar. 2013.
[18] H. Linget, T. Chanelière, J.-L. Le Gouët, and A. Louchet-Chauvet, "Time reversal of light by linear dispersive filtering near atomic resonance," *New J. Phys.*, vol. 15, Jun. 2013, Art. ID 063037.

[19] F. Coppinger, A. Bhushan, and B. Jalali, "Time reversal of broadband microwave signals," *Electron. Lett.*, vol. 35, no. 15, pp. 1230–1232, Jul. 1999.
[20] J. Zhang and J. Yao, "Broadband and precise microwave time reversal using a single linearly chirped fiber Bragg grating," in *Proc. Int. Topical Meeting on Microw. Photon. and 9th Asia–Pacific Microw. Photon. Conf.*, Oct. 2014, pp. 57–60, paper TuD-2.
[21] J. Yao, "Photonic generation of microwave arbitrary waveforms," *Opt. Commun.*, vol. 284, no. 15, pp. 3723–3736, Jul. 2011.
[22] H. Chi and J. Yao, "Symmetrical waveform generation based on temporal pulse shaping using amplitude-only modulator," *Electron. Lett.*, vol. 43, no. 7, pp. 415–417, Mar. 2007.
[23] C. Wang, M. Li, and J. Yao, "Continuously tunable photonic microwave frequency multiplication by use of an unbalanced temporal pulse shaping system," *IEEE Photon. Technol. Lett.*, vol. 22, no. 17, pp. 1285–1287, Sep. 2010.
[24] M. Weeks, "Digital signal processing using MATLAB and wavelets," *Jones and Bartlett Learning*, p. 106, 2010.
[25] F. Coppinger, A. Bhushan, and B. Jalali, "Photonic time stretch and its application to analog-to-digital conversion," *IEEE Trans. Microw. Theory Techn.*, vol. 47, no. 7, pp. 1309–1314, Jul. 1999.

Jiejun Zhang (S'12) received the B.Eng. degree in electronic science and technology from Harbin Institute of Technology, Harbin, China, in 2010, and the M.Sc. Degree in optical engineering from Huazhong University of Science and Technology, Wuhan, China. He is currently working toward the Ph.D. degree in electrical engineering and computer science at the Microwave Photonics Research Laboratory, University of Ottawa, Ottawa, ON, Canada.

His research interests include photonic generation of microwave waveforms, photonic processing of microwave signals, and fiber-optic sensors.

Jianping Yao (M'99–SM'01–F'12) received the Ph.D. degree in electrical engineering from the Université de Toulon, Toulon, France, in 1997.

He is a Professor and University Research Chair with the School of Electrical Engineering and Computer Science, University of Ottawa, Ottawa, ON, Ontario, Canada. He joined the School of Electrical and Electronic Engineering, Nanyang Technological University, Singapore, as an Assistant Professor in 1998. In December 2001, he joined the School of Electrical Engineering and Computer Science, University of Ottawa, as an Assistant Professor, where he became an Associate Professor in 2003, and a Full Professor in 2006. He was appointed University Research Chair in Microwave Photonics in 2007. From July 2007 to June 2010, he was the Director of the Ottawa-Carleton Institute for Electrical and Computer Engineering. He was reappointed Director of the Ottawa-Carleton Institute for Electrical and Computer Engineering in 2013. He has authored and coauthored more than 460 papers, including more than 260 papers in peer-reviewed journals and 200 papers in conference proceedings.

Prof. Yao is a Fellow of the Optical Society of America and the Canadian Academy of Engineering. He is a registered Professional Engineer of Ontario. He was the recipient of the 2005 International Creative Research Award at the University of Ottawa and the 2007 George S. Glinski Award for Excellence in Research. He was selected to receive an inaugural OSA outstanding reviewer award in 2012. He is an IEEE Microwave Theory and Techniques Society (MTT-S) Distinguished Microwave Lecturer for 2013–2015. He served as a guest editor for the Focus Issue on Microwave Photonics in *Optics Express* in 2013 and a Feature Issue on Microwave Photonics in *Photonics Research* in 2014. He is currently a Topical Editor for *Optics Letters*, and serves on the Editorial Board of the IEEE TRANSACTIONS ON MICROWAVE THEORY AND TECHNIQUES, Optics Communications, and China Science Bulletin. Prof. Yao is a Chair of numerous international conferences, symposia, and workshops, including the Vice Technical Program Committee (TPC) Chair of the IEEE Microwave Photonics Conference in 2007, TPC Co-Chair of the Asia–Pacific Microwave Photonics Conference in 2009 and 2010, TPC Chair of the high-speed and broadband wireless technologies subcommittee of the IEEE Radio Wireless Symposium in 2009–2012, TPC Chair of the microwave photonics subcommittee of the IEEE Photonics Society Annual Meeting in 2009, TPC Chair of the IEEE Microwave Photonics Conference in 2010, General Co-Chair of the IEEE Microwave Photonics Conference in 2011, TPC Co-Chair of the IEEE Microwave Photonics Conference in 2014, and General Co-Chair of the IEEE Microwave Photonics Conference in 2015.